Sub-microsecond optoplasmonic detection of single proteins and particles

Man, Linda de

Sub-microsecond Optoplasmonic Detection of Single Proteins and Particles

THESIS

submitted in partial fulfillment of the
requirements for the degree of

MASTER OF SCIENCE
in
PHYSICS

Author :	Linda de Man
Student ID :	s2993740
Supervisor :	N. Asgari
	Prof.dr. M.A.G.J. Orrit
Second corrector :	Prof.dr. M.P. van Exter

Leiden, The Netherlands, July 7, 2023

Sub-microsecond Optoplasmonic Detection of Single Proteins and Particles

Linda de Man

Huygens-Kamerlingh Onnes Laboratory, Leiden University
P.O. Box 9500, 2300 RA Leiden, The Netherlands

July 7, 2023

Abstract

Sub-microsecond optoplasmonic detection has been utilized to measure the interactions of single ferritin, single apoferritin, and single gold nanospheres (GNSs) with an immobilized gold nanorod (GNR) of dimensions 40 x 112 nm^2. If a protein enters the near-field region of the GNR, a redshift in localized surface plasmon resonance (LSPR) occurs, which is quantified as amplitude changes in volts (V) in the performed time trace measurements of the scattered light by the GNR. This resulted in a relative change in scattering cross section ($\Delta\sigma/\sigma$) of 1.2% and 1.9% for the mean and maximum burst amplitude of the GNS, respectively. When applying the correlation between GNS and apoferritin found with the boundary element method (BEM) simulation, an expected mean burst amplitude of 0.27 mV ($\Delta\sigma/\sigma$ = 0.24%) is anticipated, which falls within the achieved signal-to-noise ratio during the performed measurements. For ferritin $\Delta\sigma/\sigma$ was 0.73% and 1.04%, representing two measurements performed on different GNRs. These $\Delta\sigma/\sigma$ can be compared to 5.8% and 1.25% for GNS and ferritin, respectively, obtained from the BEM simulations, resulting in a good comparison between the measured and performed BEM simulations for the GNS and Ferritin.

Contents

Version of July 7, 2023– Created July 7, 2023 - 13:03

Version of July 7, 2023– Created July 7, 2023 - 13:03

Introduction

Some of the physical and chemical properties and behavior of single molecules are hidden when measured in ensemble. To recover this lost information, one applies single molecule detection techniques that allow real time measurement and recording of these behaviors and properties. Many of these phenomena occur on a microsecond time scale, such as some enzymatic reactions [1], and certain elementary steps in protein folding [2]. Studying these processes requires a technique capable of real-time detection of these dynamics on a microsecond time scale. Documenting the properties and behaviors of proteins is crucial when aiming to non-invasively and efficiently characterize the protein content of cells, for instance.

There are multiple methods for measuring single molecules, a plasmonic biosensing method is used [3]. Typically, this method relies on either the fluorescence or absorption of a single molecule by labeling it with a fluorescence dye. However, such labeling can alter the properties of the molecule and may result in blinking and/or bleaching phenomena [4]. In this thesis, a label-free refractive index-based method is used, which does not have these limitations.

This refractive index method relies on a localized surface plasmon resonance (LSPR), which is created by free-electron oscillations in metal nanoparticles (NP) when they are illuminated by a light source [5]. In the measurements conducted, a gold nanorod (GNR) is used due to its stronger enhanced E-field compared to other metal NP and because of the possibility to tune the LSPR by changing the length-to-diameter ratio of the GNR.

In this method, the GNR is probed with a specified wavelength, and a time trace signal of scattered light is recorded. When a protein approaches the near field of the GNR, it causes an increase in the local refractive index in comparison to water. This leads to a red shift of the LSPR. When the probing frequency is in the long wavelength flank of the LSPR, an increase in intensity is observed [3]. During our measurements, the protein or particles are freely diffusing, thus constantly moving in and out of the enhanced field. This movement is visualized as a spike in the time trace signal.

In this thesis, the mean amplitude of these spikes will be measured for single ferritin, single apoferritin, and single gold nanospheres (GNSs). These measurements will be compared to the results obtained from boundary element method (BEM) simulations. Although direct comparisons cannot be made, it is possible to compare relative signal amplitudes between the proteins and particles when measured on the same GNR.

The first chapter of this thesis focuses on presenting some necessary

Version of July 7, 2023– Created July 7, 2023 - 13:03

theory, including the LSPR, Interferometric scattering microscopy (iSCAT), and the diffusion coefficient. The second chapter focuses on the setup, sample preparation, alignment, and time trace recordings. The third chapter presents the results obtained in this thesis including BEM simulation and the mean amplitude bursts for single ferritin, single apoferritin, and single GNSs. The last chapter concludes and summarizes the main results of this research.

Chapter 1

Theory

To interpret the signals from nanoparticles (NPs) and their interactions, some background theory is needed. We start by explaining the localized surface plasmon resonance (LSPR) and the scattering cross section. After this, an advanced imaging technique, called interferometric scattering microscopy (iSCAT), is discussed. Lastly, the diffusion coefficient is explained.

1.1 Localized surface plasmon resonance

Localized surface plasmons (LSPs) occur when a metal NP is irradiated by light. The conduction electrons in the NP will start to coherently oscillate with the electric field of the light, this is known as a LSP. When the excitation frequency and the eigenfrequency match, the oscillating conduction electrons reach a resonance, known as localized surface plasmon resonance (LSPR)[5].

The LSP has two important properties, that are used for imaging in this thesis. The first is the enhancement of the electric field near the surface of the NP and the second is that the LSPR can be excited by visible light and tuned when changing the NP shape and size. This leads to strong absorption and scattering at the maximum of the LSPR. These effects can increase the optical signals from small objects, such as proteins, making it possible to study and detect them individually. In this thesis, they are measured using the change in the LSPR peak [6]. This is possible because the location of the LSPR peak is highly affected by the refractive index of the particles.

1.2 Scattering cross section

During the following calculation the gold nanorod (GNR) is modelled as an ellipsoid, having its long axis parallel to the x-direction. With these assumptions the induced dipole moment in the three principal axes (x, y, z) can be defined as:

$$\begin{pmatrix} p_x \\ p_y \\ p_z \end{pmatrix} = \begin{pmatrix} \alpha_1 & 0 & 0 \\ 0 & \alpha_2 & 0 \\ 0 & 0 & \alpha_3 \end{pmatrix} \begin{pmatrix} E_{0x} \\ E_{0y} \\ E_{0z} \end{pmatrix} \tag{1.1}$$

Where E_{0x}, E_{0y}, and E_{0z} are the components of the applied field, and α_1, α_2, and α_3 are the principle values of the polarizability tensor of the ellipsoid. The polarizability of an ellipsoid in the Rayleigh approximation can be described by:

$$\alpha_i = 4\pi abc \frac{\epsilon - \epsilon_m}{3\epsilon_m + 3L_i(\epsilon - \epsilon_m)} \tag{1.2}$$

where a, b, and c give the dimensions of the ellipsoid along the three principle axes and ϵ_m is the permittivity of the surrounding medium. L_i is a geometrical factor given by[7]:

$$L_i = \frac{abc}{2} \int_0^{\inf} \frac{dq}{(a_i^2 + q) f(q)}, \tag{1.3}$$

where a_i is either a, b, or c one of the ellipsoid dimensions along a principle axes, $f(q) = \sqrt{(q+a^2)(q+b^2)(q+c^2)}$, where q is the charge. The geometrical factor satisfies $\sum L_i = 1$. A second coordinate system is created, chosen to be fixed relative to the incident beam, given by x', y', and z'. A formula for the scattering cross section can be obtained, in this case the light is x'-polarized.

$$C_{sca,x'} = \frac{k^4}{6\pi}(|\alpha_1|^2 a_{11}^2 + |\alpha_2|^2 a_{21}^2 + |\alpha_3|^2 a_{31}^2), \tag{1.4}$$

where $k = 2\pi/\lambda$ the wavenumber, $a_{11} = \hat{\boldsymbol{e}}_{\boldsymbol{x}} \cdot \hat{\boldsymbol{e}}_{\boldsymbol{x'}}$, $a_{21} = \hat{\boldsymbol{e}}_{\boldsymbol{y}} \cdot \hat{\boldsymbol{e}}_{\boldsymbol{x'}}$, $a_{31} = \hat{\boldsymbol{e}}_{\boldsymbol{z}} \cdot \hat{\boldsymbol{e}}_{\boldsymbol{x'}}$. All other terms are omitted because of the lights polarization. The applied field direction was chosen to be along the z-axis, this results in the third term being more dominant[8].

If the scattering cross section is calculated/measured over a wavelength range, a Lorentzian curve is expected. This correlates to the expected spectra of the GNR, where the maximum of this scattering cross section occurs at the LSPR of the GNR.

Version of July 7, 2023– Created July 7, 2023 - 13:03

1.3 Interferometric scattering microscopy (iSCAT)

Interferometric Scattering Microscopy (iSCAT) is an advanced imaging technique that provides an interferometric measurement of the electric field scattered by a small object. It allows for the visualization and characterization of individual nanoparticles and large molecules such as proteins with high sensitivity and precision[3].

Here are the key steps for imaging with iSCAT. Start by illuminating the sample, typically by using a laser. This light will interact with the sample, causing scattering. This scattered light will interfere with a reference wave, such as the transmitted wave, the reflected wave, or any auxiliary wave coherent with the illumination, and the interference pattern is detected. A high-sensitivity detector, such as a photodiode or sensitive camera, is employed for this purpose.

The imaging principle behind iSCAT is based on the interference of a scattered light wave with a reference wave. The interference signal is captured and analyzed to extract information about the sample, such as its size, position, and refractive index. This interference signal can be described by [9]:

$$I_{det} \propto |\overline{E_r} + \overline{E_s}|^2 = I_r + I_s + 2E_r E_s \cos\phi, \tag{1.5}$$

where $\overline{E_s} = E_s e^{i\phi_s}$ is the field scattered from the sample, $\overline{E_r} = E_r e^{i\phi_r}$ is the complex electric field of the reference wave, the intensity of the reference wave $I_r = |\overline{E_r}|^2$, the intensity of the scattered wave $I_s = |\overline{E_s}|^2$, and lastly the cross term of the two waves containing $\phi = \phi_r - \phi_s$.

The main advantage of iSCAT is its high sensitivity to changes in the refractive index and size of nanoparticles or molecules. It scales with the partical size (r) as r^3, whereas the dark field scattered intensity scales as r^6. Therefore, it provides better sensitivity for small particles. It can detect and visualize particles as small as a few nanometers and provide quantitative measurements of their properties. It also allows for the study of individual particles and their interactions in real-time.

1.4 Diffusion coefficients

We can make the assumption that the protein behaves as a sphere undergoing random motion, known as Brownian motion. The covered distance (L) in each elementary step of the random walk is equal to the speed of the particle (v) times the typical duration (Δt) of the step. The mean squared displacement is defined as $L^2 = Dt$, where D is the diffusion coefficient.

Version of July 7, 2023– Created July 7, 2023 - 13:03

When a particle is at random walking through the fluid it experiences a certain amount of frictional force, called the Stokes drag force defined as:

$$F = 6\pi\mu R\nu \tag{1.6}$$

Where μ is the viscosity of the fluid, ν the traveling speed, R the radius of the sphere. The typical energy dissipated or absorbed for one such Brownian motion step is equal to the thermal Boltzmann energy:

$$k_b T = FL, \tag{1.7}$$

where k_b is Boltzmann's constant and T is the temperature. We thus deduce the Stokes Einstein relation and find the diffusion coefficient[10]:

$$D = \frac{L^2}{\Delta t} = \frac{k_b T}{6\pi\mu R} \tag{1.8}$$

Chapter 2

Method

2.1 Confocal setup

All separate elements used in the setup are listed in Appendix A. The setup is used with two different light sources, a white-light source, and a tunable light source (785 $\pm$ 25 nm).

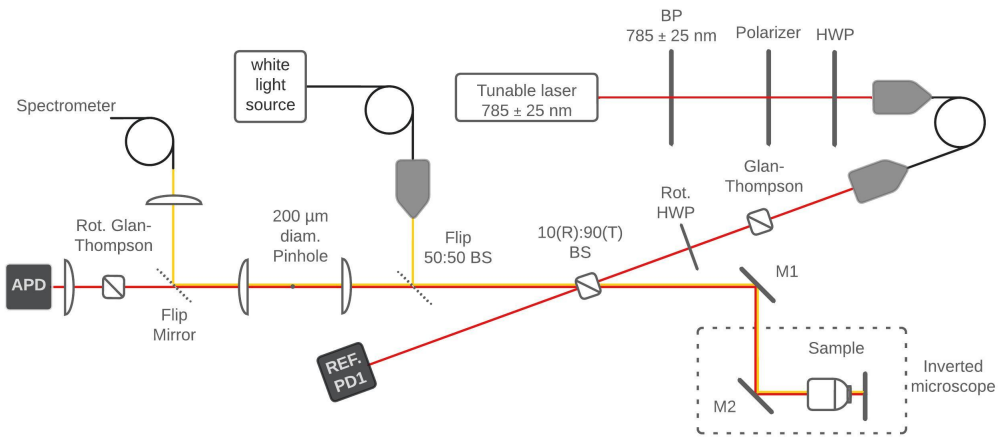

Figure 2.1: *Schematic image of the setup. Using the white-light source (yellow line) we are able to measure the gold nanorod (GNR) spectra using the spectrometer to find the resonance wavelength. The tunable laser (red) is used to locate/image the GNR and detect its change in localized surface plasmonic resonance (LSPR) over time, with high accuracy.*

The tunable laser is used for imaging the gold nanorods (GNRs), finding their polarization orientation and perform time trace measurements.

The tunable laser light first goes through a bandpass (BP) filter (785 $\pm$ 25 nm) and then a polarizer (used for tuning the intensity). After the polarizer it will go through a single mode polarization-maintaining optical fiber and a Glan-Thompson prism. Now that the light has a specified polarization orientation it will go through a half-wave plate (HWP) to change this polarization to any specified angle. This HWP together with the rotatable Glan-Thompson prism (located further in the setup) is used for creating either linear or crossed polarized interference. After the HWP the light is 10% reflected and 90% transmitted by a beam splitter (BS). The transmitted light will reach a photodiode (PD), allowing us to know the laser light intensity impinging the GNRs during the measurements. The reflected light beam goes through the objective and illuminates the sample by redirection of two silver mirrors. The light goes back the same path, is then focused and goes through a pinhole of diameter 200 μm. Lastly it is collimated again and detected with the avalanche photodiode, after passing through the rotatable Glan-Thompson prism.

The white-light source is used when measuring the spectra of the GNRs, from which we can extract the LSPR and choose the probing frequency of the laser. When using this light source both the flippable beam splitter (BS) and mirror are inserted in the setup. The white-light source goes through a multi-mode fiber and is directed at the flippable 50:50 BS. Then the light goes through a 10(R):90(T) BS and is directed by two silver mirrors through the objective onto the sample. The objective focuses the light on a single GNR of the prepared sample whose spectrum we want to visualize. The light goes back the same path until it reaches the 50:50 flippable BS. Then it is focused and goes through a pinhole with a diameter of 200 μm. After it is collimated again the light is directed by a flippable mirror and multi-mode fiber, on to the spectrometer where it is measured.

2.2 Gold nanorod immobilization

GNR are purchased from Nanopartz [11] in a CTAB solution, which is used to stabilize the growth of the GNR and make sure they will not stick to one another. The average size of the GNR was 40 x 112 nm^2 in diameter and length respectively. The expected localized surface plasmon resonance (LSPR) is 750 nm.

The first step in the GNR immobilization is diluting the sample and washing away the CTAB by centrifuging. After centrifuging, the GNR are resuspended in water and sonicated (40 min). At the same time the coverslips are ozone cleaned (1 hour), they have been sonicated beforehand in

Version of July 7, 2023– Created July 7, 2023 - 13:03

acetone (20 min) and ethanol (15 min). Next the coverslips are placed on the spin coating machine and the GNR solution is pipetted on top. After spin coating the sample is ozone cleaned again for immobilization of the GNR to the coverglass. Lastly the coverglass is slightly heated, resulting in a better immobilization process, and placed in the holder.

A full step-by-step description of all the mentioned parts is given in Appendix B.

2.3 Expected particle concentrations

In this section, we determine the needed concentration to have one molecule/protein at a time in the near field of the GNR. In this thesis single ferritin, single apoferritin, and single GNSs are measured. An image of apoferritin (ferritin without an iron core) is shown in Figure 2.2. Ferritin has an outer layer with a diameter 12 nm and an inner core diameter of 8 nm. The expected concentration needed to measure single proteins/particles is determined by using the enhanced E-field around the GNR tip.

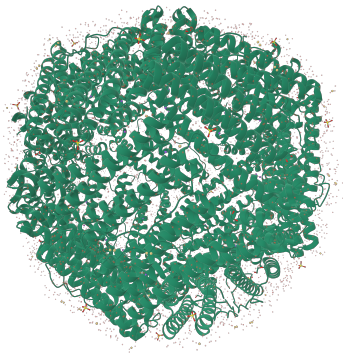

Figure 2.2: *Apoferritin structure (protein data bank code number: 6MSX)[12]*

The enhanced E-field area is determined from boundary element method (BEM) simulations, using the MNPBEM toolbox in MATLAB[13]. By estimating the enhanced E-field volume around the tip of the rod, this field is shown in figure 2.3. This volume is circularly located around the tip of the GNR, making the approximation based on spheres and cones. During this the enhanced E-field layer is determined to be around 20 nm thick, resulting in a volume of 0.001 fL. This leads to a de-

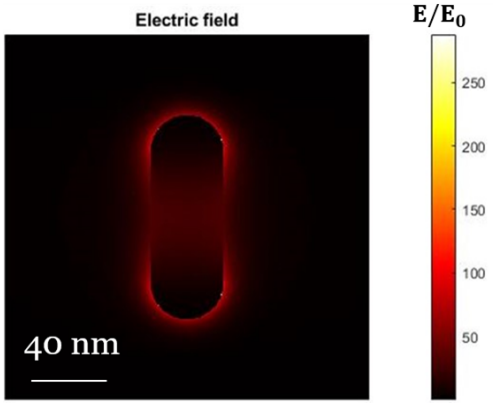

Figure 2.3: *Enhanced E-field of a GNR with dimensions 112 x 40 nm^2 in length and diameter.*

sired concentration of 1.66 μM, which should ensure that only one protein/molecule is present at a time in the near-field of the GNR.

2.3.1 Apoferritin

Apoferritin is bought in solid form, having a molecular weight of 460 kDa. 12 mg of apoferritin will be dissolved in 1000 μL of water containing NaCl (50 mM).

$$\frac{12 \text{ mg/mL}}{460 \text{ kDa}} = 26 \frac{\mu\text{mol}}{\text{L}} \tag{2.1}$$

When adding apoferritin to the sample, a ratio of 1:16 of apoferritin to water is desired, to have one apoferritin protein at a time in the near-field of the GNR.

2.3.2 Gold nanosphere

Gold nanospheres (GNS's) with a diameter of 10 nm are bought in the form of water suspension. The solution had a molarity of $8.27 * 10^{-3}$ μM, requiring the use of 200 μL of NS solution to achieve the desired concentration, to have one GNS protein at a time in the near-field of the GNR.

2.3.3 Ferritin

Ferritin is bought in the form of water suspension, containing 125 mg/mL [14]. Determining the molar weight of ferritin poses a challenge due to the unknown composition of its core. However, it is known to consist of magnetite (Fe_3O_4, 231.5 Da), ferrihydrite ($FeHO_2$, 168 Da), and hematite (Fe_2O_3, 160 Da) [15].

Due to the exact ratio of the components being not precisely known for each individual molecule, the average has been taken, resulting in a molecular weight of 186.8 Da. To get the total molar weight of the core this needs to be multiplied by the amount of iron ions. The amount of iron ions is equal to 4500 and the three components have an average number of 2.33 iron ions. This gives a molecular weight of 360 kDa for the core. The total molecular weight of ferritin is 800 kDa, because the molecular weight without the core was given as 440 kDa.

$$\frac{125 \text{ mg/mL}}{800 \text{ kDa}} = 156 \frac{\mu\text{mol}}{\text{L}} \tag{2.2}$$

When adding ferritin to the sample, a ratio of 1:94 of ferritin to water is desired, to have one GNS protein at a time in the near-field of the GNR.

Version of July 7, 2023– Created July 7, 2023 - 13:03

2.4 Alignment

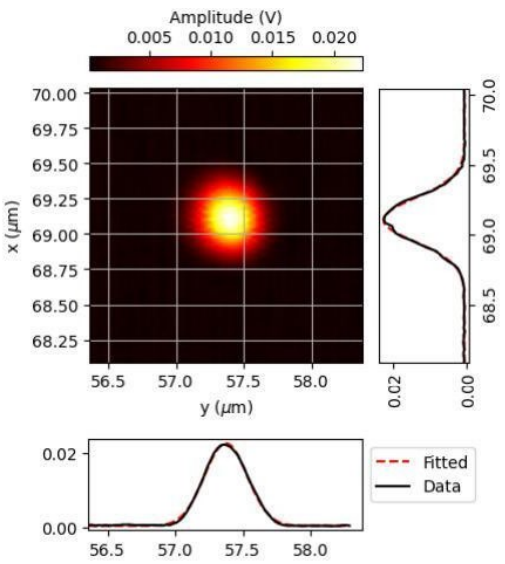

(a) *xy-image*

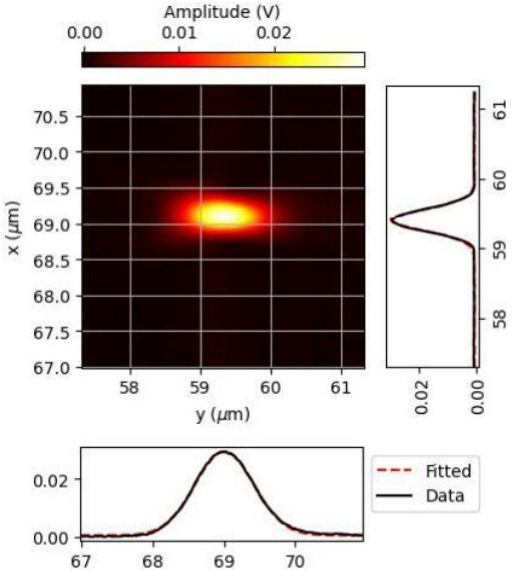

(b) *xz-image*

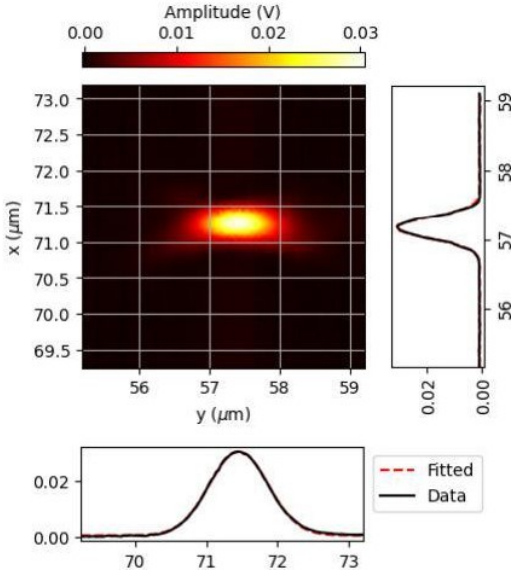

(c) *yz-image*

Figure 2.4: *2D scans of a single gold nanorod (GNR) with (a) xy-orientation (b) xz-orientation and (c) yx-orientation. Each subfigure shows this 2D scan with a Gaussian-fitted plot next to it, which is performed on the data that goes through the maximum intensity point of the GNR along one of the principle axes (x, y, or z).*

The alignment of the setup is checked by using the point spread function (PSF). This PSF for a well-aligned confocal setup has a 2D Gaussian profile. To check the PSF GNRs with a diameter of 40 nm and length of 112 nm have been used. If the shape does not agree with the expected PSF, the pinhole and tube lens before the pinhole can be slightly adjusted. Then,

the PSF is rechecked to determine if it exhibits the anticipated 2D Gaussian profile. The final PSFs of our confocal setup are shown in figure 2.4.

In figure 2.4c a 2D amplitude scan of the xy direction is visualized, this scan is expected to exhibit a symmetric Gaussian distribution. In order to assess the alignment, a Gaussian fitting procedure is executed on extracted data. This data is along both principal axis in each figure and goes through the maximum intensity point. These plots are shown next to the 2D amplitude scan.

2.5 Time trace recordings

The mounted sample is brought into focus, by checking the laser intensity and moving the sample slowly down. When in focus an image of around 50 μm x 50 μm is made to visualize the location of the GNRs in that region. Then the GNRs ($\approx$ 20) are marked, by checking the location at which the intensity is maximum.

Before starting the time trace measurements, the polarization and spectra of the GNRs are visualized. The polarization is determined with the use of the red laser, by gradually changing the rotatable HWP and Glan-Thompson prism from 0 to 180 degrees. This will provide the polarization orientation of the GNRs, during the measurement both are placed on the found maximum angles for maximizing signal-to-noise ratio. When measuring the spectra of a GNR the laser light is turned off and the white-light source is used. Also, both the flippable mirror and the flippable BS are inserted into the setup. This light source illuminates the GNR and measures its spectra with the spectrometer, this spectra is expected to be of Lorentzian shape. From this, the LSPR of the GNRs and the set probing frequency of the laser are determined.

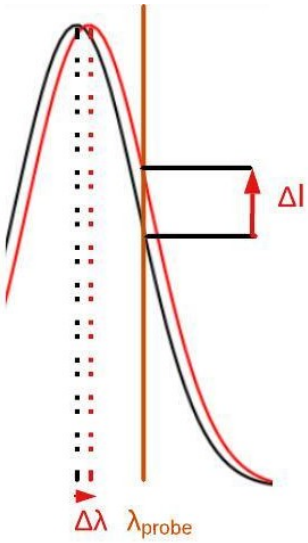

Figure 2.5: *Visualizes the redshift (red) of the original spectra (black), and the corresponding increase in amplitude (blue). This increase correlates to the peaks in the time trace measurements.*

From both the polarization and spectra one or more GNRs are chosen, based on being within the probing range of the

tuneable laser and the Lorentzian shape of the spectra. Time trace measurements can now be performed, in the case of this thesis traces of duration 10 ms are recorded at a sampling rate of 0.2 ns. The GNR is always probed on the long wavelength flank of the LSPR. When a particle enters the near field of the GNR a redshift occurs to the spectra as visualized in figure 2.5. This red shift will result in a temporary increase in the amplitude of the time trace signal, making it possible to correlate the entering/leaving of a protein/molecule in the enhanced E-field to the peaks in the time trace signal.

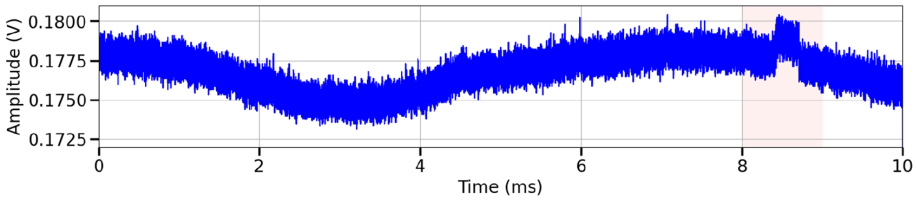

Figure 2.6: *An time trace example for a ferritin burst of duration 10 ms at a sampling rate of 0.2 ns.*

Chapter 3

Results and discussion

This chapter commences with a discussion of the outcomes obtained from the boundary element method (BEM) simulation, focusing on the correlation in mean amplitude among different proteins and particles. Then, the results of a gold nanosphere (NS) are presented. Finally, the measurement results obtained using ferritin are discussed.

3.1 Boundary element method simulations

Boundary element method (BEM) simulations using the MNPBEM library from MATLAB are performed for each system[13]. The first system is the interaction of ferritin with a gold nanorod (GNR) of dimension 40 x 112 nm^2, diameter by length respectively. The second system is the interaction of apoferritin with the same GNR. The last system is the interaction of a gold nanosphere (GNS) again with the same GNR. In each simulation, the protein/particle is placed along the GNR's long axis at a specified distance d from the tip. This setup is visualized in Figure 3.2d. For the simulation, several refractive index

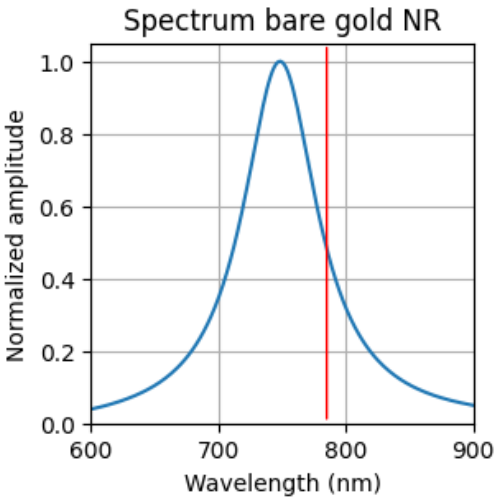

Figure 3.1: *Bare GNR spectra, with LSPR of 749 nm, and the probing frequency is visualized by the red line at 785 nm.*

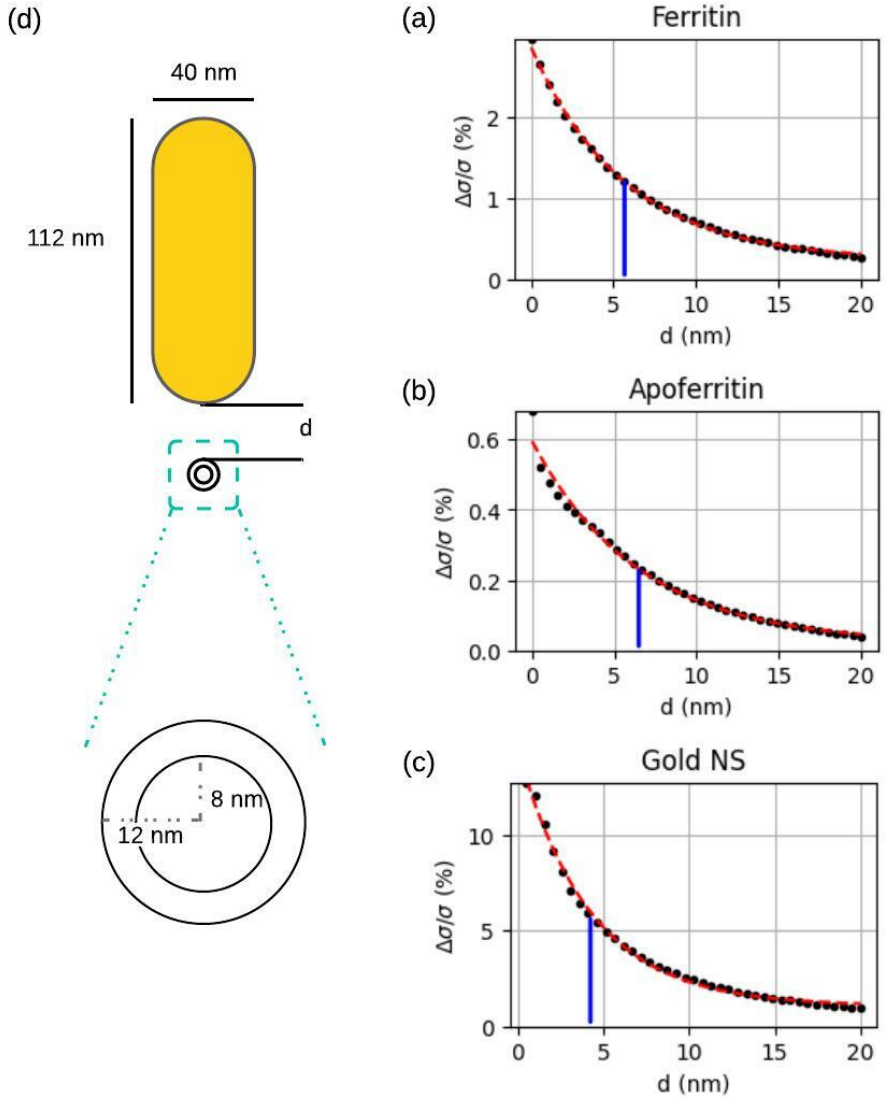

Figure 3.2: *(a), (b), and (c) show the scattering cross section as a function of displacement d, for ferritin, apoferritin, and a Gold NS respectively. Obtained from a Boundary Element Method (BEM) simulation conducted using MATLAB. The red curve is a fitted exponential decay function, and the blue straight line represents the decay length (1/e). The setup used for these BEM simulations is shown in (d)*

values are required. The refractive index for water is assumed to be 1.33, while the refractive index of the ferritin layer is set to 1.5. It should be noted that the refractive indices of gold and the ferritin core are strongly wavelength dependent. Due to the core composition, the refractive index

of hematite has been used[16].

The BEM simulation will return a spectrum ($\sigma_k(\lambda)$) as a function of wavelength (λ). This spectrum can then be compared with the spectra for a bare GNR ($\sigma_0(\lambda)$), to determine the relative change in scattering cross section ($\Delta\sigma/\sigma$).

$$\frac{\Delta\sigma_i}{\sigma} = |\sigma_k(\lambda) - \sigma_0(\lambda)|/\sigma_0(\lambda) \tag{3.1}$$

The LSPR of the bare GNR is determined to be 749 nm, this agrees with the specification. From this LSPR a probing frequency of 785 nm is chosen, which is on the long wavelength flank of the spectra. Figure 3.2a, 3.2b, and 3.2c show the determined relative changes in scattering cross section as the distance between the GNR and protein/particle (Ferritin, apoferritin, and GNS respectively) is increased.

All graphs can be described by an exponential decay function which allows us to obtain the decay length d_l. The found d_l is 5.66 nm, 6.48 nm, and 4.24 nm for ferritin, apoferritin, and a GNS respectively. Using these values as root mean squared (rms) displacement, relative changes in the scattering cross section can be determined ($\Delta\sigma_i/\sigma$). $\Delta\sigma_i/\sigma$ is 1.25, 0.24, and 5.8 % for ferritin, apoferritin, and the GNSs respectively. From this we can create two relations:

$$\frac{\Delta\sigma_{NS}}{\Delta\sigma_F} = 4.64 \tag{3.2}$$

and

$$\frac{\Delta\sigma_{NS}}{\Delta\sigma_{ApoF}} = 24.2 \tag{3.3}$$

These relations will be used to compare the expected protein/particle signal with each other.

3.2 Mean amplitude of the gold nanospheres

Prior to the measurement, the spectra and polarization of the GNRs are examined. The used GNR spectra is presented in Appendix C. The LSPR of NR1 before the measurement is 750 nm. The probing frequency used during the measurement is equal to 785 nm. The incident power during the measurements was ≈ 100 μW on the GNR.

The final solution used for the GNS was 600 μL, together with 30 μL PBS. This concentration of GNS is 3 times higher than the calculated concentration in chapter 2.3.2, resulting in 4.73 μM. An example time trace for a gold NS is shown in figure 3.3. This figure displays clear bursts with sharp spikes. These bursts are analyzed with a LabVIEW code. This code

normalizes the trace around 0 and is then able to select the bursts (using a threshold). A burst is defined from the moment it enters the near field until it leaves the near field. From these bursts mean amplitude are determined. All these mean amplitudes are plotted as a histogram in figure 3.6a. Over this histogram plot, Gaussian fits are performed resulting in a maximum at 3.00 mV for the mean burst amplitude. It is anticipated that the mean burst amplitude of the GNSs will not serve as a reliable correlation parameter to ferritin due to the difference in burst duration. As a result, the maximum values of the bursts are also determined and plotted in the same manner as visualized in Figure 3.6b, with the highest value found at 4.82 mV.

Using these mean burst amplitude values, the relative change in scattering cross-section ($\Delta\sigma/\sigma$) can be approximated. For this purpose, a reference signal of 0.253 V was used, resulting in a relative change in scattering cross-section of 1.2% based on the mean burst amplitude value. If the maximum burst amplitude value is used, the relative change increases to

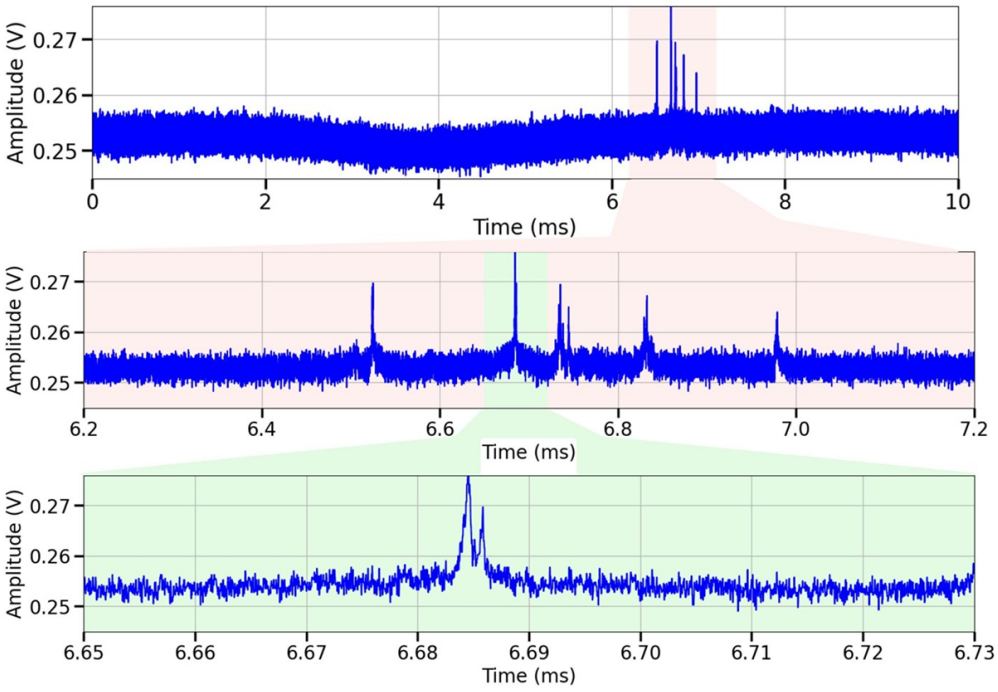

Figure 3.3: *The first graph displays a example of a time trace for GNS interaction with a GNR. The second and third graph provides a zoomed-in view of the bursts. The GNS concentration is 4.73 μM.*

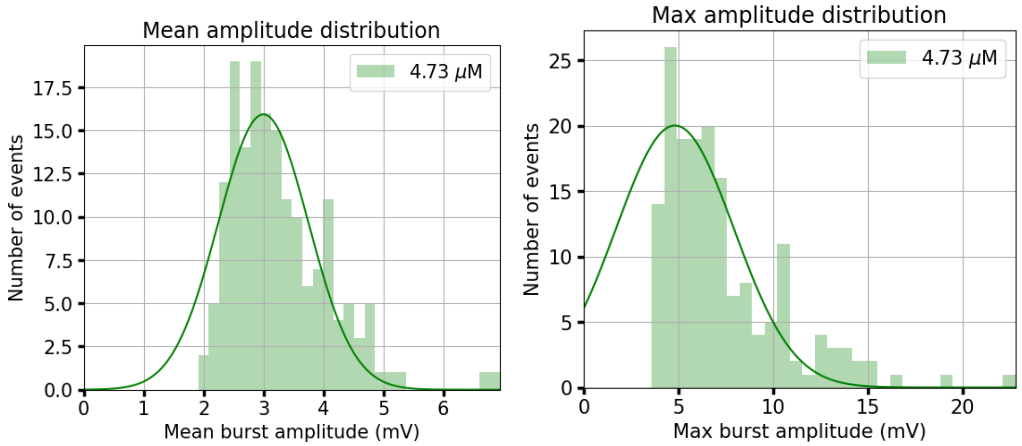

(a) *Mean burst amplitude* ***(b)*** *Maximum of the burst amplitudes*

Figure 3.4: *Histogram of the mean (a) and maximum (b) amplitude with a fitted Gaussian function. A total of 169 bursts were recorded using 4.73 μM quantities of gold NS, resulting in a maximum at 3.0 mV and 4.8 mV for the mean and maximum amplitude respectively.*

1.9%. These values can be compared to the 5.8% obtained from the BEM simulation, this shows a large decrease in measured $\Delta\sigma/\sigma$ compared to the BEM simulations. This change can be explained by the citrate/CTAB left on the GNS/GNR, this effect the distance it is able to enter the near field. Additionally, the GNS exhibits a slight distribution in sizes.

3.3 Mean amplitude of ferritin

Prior to the measurement, the spectra and polarization of the gold nanorod (GNR) is examined. The used GNR spectra is presented in Appendix C. In this section, two measurement sets were conducted on different GNRs with varying concentrations of ferritin. The LSPR of NR2 before the measurement is 758 nm and after 767 nm. The LSPR of NR3 remains unchanged and is 770 nm. The slight LSPR increase in NR2 might indicate that ferritin is sticking to the GNR, but it can be neglected in our case due to the small magnitude of this increase. The probing frequency used for both measurement sets is equal to 788 nm. The used incident power on NR2 was ≈ 60 μW and on NR3 ≈ 100 μW.

Now on top of the sample a solution is placed. The solution has a concentration of 0.86 μM and 1.39 μM of ferritin for NR2 and NR3 respectively. During the measurement time trace signals are saved, such a signal

is visualized in figure 3.5. In the first graph a typical time trace signal is given, this has a duration of 10 ms at a sampling rate of 0.2 ns. The second graph zooms in on 8 - 9 ms of the first graph, here a burst is visualized. These bursts are analyzed with a LabVIEW code, during this thesis some changes have been made to the code, these are discussed and validated in appendix D.

This code normalizes the trace around 0 and is then able to select the bursts and determines their mean amplitude. All these mean amplitudes are plotted in figure **??** and **??** for NR2 and NR3 respectively.

Over these histogram plots, Gaussian fits are performed resulting in maximums at 1.3 mV and 1.5 mV in mean burst amplitude for the 0.86 μM and 1.39 μM quantities of ferritin respectively. There is no correlation between the burst maximum and the concentration used, this concentration only affects the number of burst occurrences in a certain time frame.

Using these mean burst amplitude values, the relative change in scattering cross-section ($\Delta\sigma/\sigma$) can be approximated. For this purpose, a reference signal of 0.177V and 0.135 V was used for NR2 and NR3 respectively, giving $\Delta\sigma/\sigma$ as 0.73% and 1.04%. These values can be compared to the 1.25% obtained from the BEM simulation. The $\Delta\sigma/\sigma$ values for the GNS and ferritin are shown in table 3.1. Based on the $\Delta\sigma/\sigma$ values, it can be concluded that ferritin exhibits a stronger correlation to the simulation compared to the GNS. This difference in correlation could be attributed to the measured burst durations or the nature of the interactions involved.

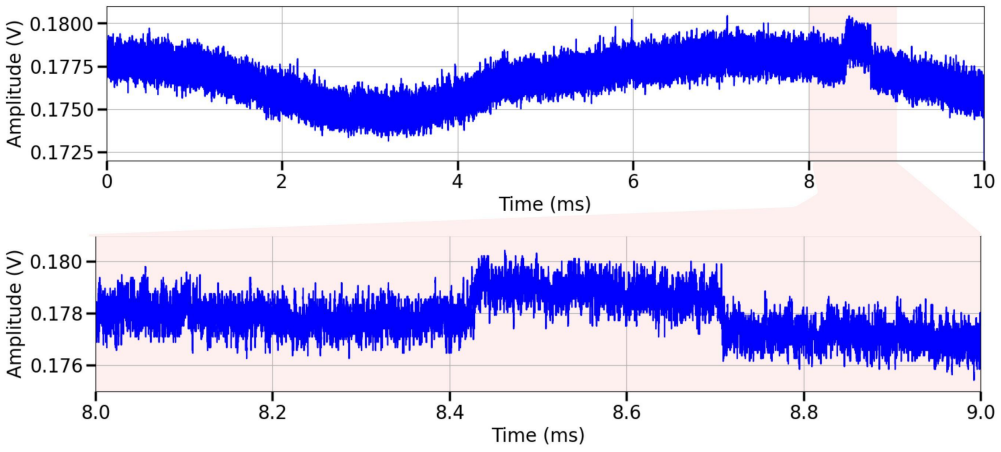

Figure 3.5: *Shows a typical trace for these GNR in the above graph, the second graph is a zoom-in on the burst. The sample during this trace has a concentration of 0.86 μM ferritin*

The GNS rapidly approaches the near-field at various distances, leading to a wider range of mean/maximum burst amplitudes. On the other hand, ferritin adheres to the GNR, ensuring a consistent distance in each measurement, and the observed variations are caused by different locations of adherence on the GNR.

$\Delta\sigma/\sigma$ (%)	0.86μM ferritin	1.39 μM ferritin	mean GNS	max GNS
BEM simulations	1.25	1.25	5.8	5.8
measured	0.73	1.04	1.2	1.9

Table 3.1: *Shows the relative change in scattering cross section ($\Delta\sigma_k$), measured compared to simulated in percentage.*

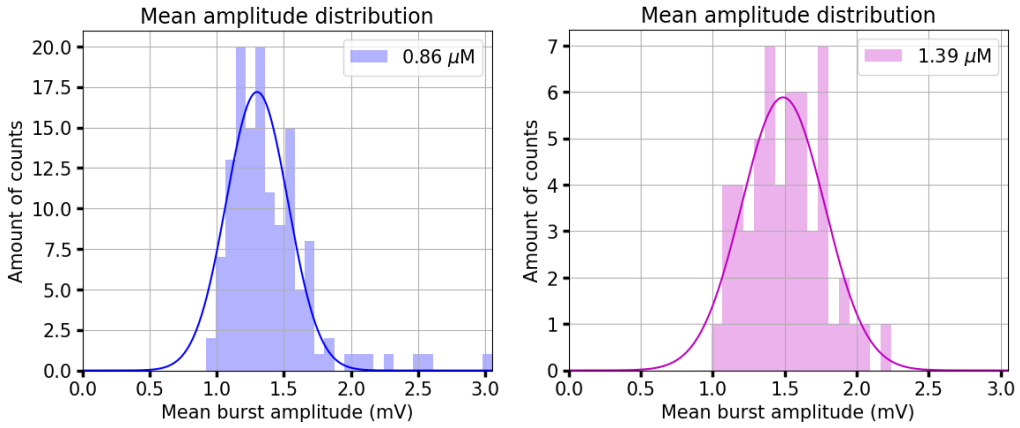

(a) *A total of 135 bursts* ***(b)*** *A total of 56 bursts*

Figure 3.6: *Histogram of the mean amplitude with a fitted Gaussian function, having a maximum at 1.3 mV and 1.4 mV for 0.86 μM (a) and 1.39 μM (b) of ferritin respectively.*

Apoferritin has been measured on NR2, resulting in nearly no visible burst and the burst visible are in the order of 0.9 mV, $\approx$ 3 bursts have been detected. During the initial stages of trace analysis, it became evident that there would be an insufficient amount of apoferritin burst available for comparison with ferritin. Even if there were enough bursts, they would not provide an accurate representation due to signals below approximately 0.7 mV being concealed within the current signal-to-noise ratio. When applying the relations from the BEM simulation and the found mean burst amplitude of ferritin, a mean burst amplitude of 0.27 mV is expected for apoferritin.

Lastly, the measured relative change in scattering cross section $\Delta\sigma/\sigma$ of ferritin can be compared to that for GNSs. This results in 1.36 and 2.15 depending if the mean or max amplitude burst value of the GNS has been taken, respectively. These values can be compared to the 4.64 found with the BEM simulations. Although the maximum burst amplitude is closer to the expected ratio, there is still a deviation. This deviation could be caused by various factors, including the median filter applied to the data before determining the maximum value, the approximation made when simulating the ferritin core, the measurements being conducted on different GNRs, the CTAB/citrate layer minimizing entrance into the near-field, or the fact that these layers have not been included in the simulations.

Chapter 4

Conclusion

The expected change in scattering cross section was determined using the MNPBEM library in MATLAB. This research focusses on the interaction between a gold nanorod (GNR) of dimension 40 x 112 nm^2 and different proteins/particles. The localized surface plasmon resonance (LSPR) for this bare GNR is 749 nm which agrees with the specified value of 750 nm. Simulations were conducted for single ferritin, single apoferritin, and single gold nanosphere (GNS) by varying the tip-to-tip distance along the long axis of the GNR. This revealed decay lengths d_l of 5.66 nm, 6.48 nm, and 4.24 nm for ferritin, apoferritin, and GNSs respectively. Using these values as root mean squared (rms) displacement, relative changes in the scattering cross section ($\Delta\sigma/\sigma$) can be determined as 1.25, 0.24, and 5.8% for ferritin, apoferritin, and a gold NS respectively.

Using the mean burst amplitude values, the relative change in scattering cross-section can be approximated. Resulting in 1.2% and 1.9% for the GNSs when using the mean and maximum burst values respectively. For ferritin 0.73% and 1.04% were found when using 0.86 μM and 1.39 μM quantities of ferritin respectively. These relative changes in scattering cross section can be compared to 5.8% and 1.25% for GNSs and ferritin, respectively, obtained from the simulations. The deviation for the GNSs is larger than for ferritin. This deviation could be caused by various factors, including the median filter applied to the data before determining the maximum value, the approximation made when simulating the ferritin core, the measurements being conducted on different GNRs, the CTAB/citrate layer minimizing entrance into the near-field, or the fact that these layers have not been included in the simulations.

The measured relative change in scattering cross section $\Delta\sigma/\sigma$ of ferritin can be compared to that for GNSs. This results in 1.36 and 2.15 de-

pending if the mean or maximum burst amplitude values of the GNS have been taken, respectively. These values can be compared to the 4.64 found with the BEM simulations. This deviation is caused mostly by the earlier stated deviation in $\Delta\sigma/\sigma$ for the GNS.

Apoferritin has been measured which gave nearly no visible burst and the burst visible are in the order of 0.9 mV. Approximately 3 bursts were detected, this would be an insufficient amount of apoferritin burst for statistical analysis. These bursts are also not an accurate representation due to signals below approximately 0.7 mV being concealed within the current signal-to-noise ratio. When applying the relations from the BEM simulation a mean burst amplitude of 0.27 mV ($\Delta\sigma/\sigma$ = 0.24%) is expected for apoferritin.

In this work we were able to find a good comparison between the measured and the performed BEM simulation of GNSs and ferritin. If the signal to noise ratio is improved, by for example increasing the laser intensity and/or optimizing the detectors amplification settings, measuring apoferritin could be within reach.

Version of July 7, 2023– Created July 7, 2023 - 13:03

Acknowledgements

First of all, I would like to express my gratitude to Michel Orrit for providing me with this amazing opportunity. Under the guidance of Nasrin Asgari, I had the chance to immerse myself in the fascinating field of single protein detection, where I acquired valuable knowledge and learned completely new things. I would like to extend my sincere thanks to Nasrin Asgari for her guidance throughout this journey.

I would also like to express my thanks to Martin Baakse for his helpful comments and feedback on the obtained measurement results. Lastly, I would like to acknowledge and thank everyone in the QMO and MoNOS groups. Their helpful information, feedback, and discussions have played a significant role in shaping the outcomes of this project.

Bibliography

[1] R. M. Daniel, J. L. Finney, V. Reat, R. Dunn, M. Ferrand, and J. C. Smith, "Enzyme dynamics and activity: Time-scale dependence of dynamical transitions in glutamate dehydrogenase solution," *Biophysical Journal*, vol. 77, no. 4, pp. 2184–2190, 1999. [Online]. Available: https://www.sciencedirect.com/science/article/pii/S000634959977058X

[2] O. Bieri and T. Kiefhaber, "Elementary steps in protein folding," vol. 380, no. 7-8, pp. 923–929, 1999. [Online]. Available: https://doi.org/10.1515/BC.1999.114

[3] M. D. Baaske, N. Asgari, D. Punj, and M. Orrit, "Nanosecond time scale transient optoplasmonic detection of single proteins," *Science Advances*, vol. 8, no. 2, p. eabl5576, 2022. [Online]. Available: https://www.science.org/doi/abs/10.1126/sciadv.abl5576

[4] D. T. Burnette, P. Sengupta, Y. Dai, J. Lippincott-Schwartz, and B. Kachar, "Bleaching/blinking assisted localization microscopy for superresolution imaging using standard fluorescent molecules," *Proceedings of the National Academy of Sciences*, vol. 108, no. 52, pp. 21 081–21 086, 2011. [Online]. Available: https://www.pnas.org/doi/abs/10.1073/pnas.1117430109

[5] E. Petryayeva and U. J. Krull, "Localized surface plasmon resonance: Nanostructures, bioassays and biosensingâa review," *Analytica Chimica Acta*, vol. 706, no. 1, pp. 8–24, 2011. [Online]. Available: https://www.sciencedirect.com/science/article/pii/S0003267011011196

[6] K. M. Mayer and J. H. Hafner, "Localized surface plasmon resonance sensors," *Chemical Reviews*, vol. 111, no. 6, pp. 3828–3857, 2011, pMID: 21648956. [Online]. Available: https://doi.org/10.1021/cr100313v

[7] S.A.Maier, *Localized Surface Plasmons*. Springen, 2007, ch. 5.

[8] *Particles Small Compared with the Wavelength*. John Wiley Sons, Ltd, 1998, ch. 5, pp. 130–157. [Online]. Available: https://onlinelibrary.wiley.com/doi/abs/10.1002/9783527618156.ch5

[9] R. W. Taylor and V. Sandoghdar, *Interferometric Scattering (iSCAT) Microscopy and Related Techniques*. Cham: Springer International Publishing, 2019, pp. 25–65. [Online]. Available: https://doi.org/10.1007/978-3-030-21722-8_2

[10] M. A. G. J. Orrit, "Lecture notes in single molecule optics," March 2022.

[11] "Gold nanorods properties, applications, and products." [Online]. Available: https://www.nanopartz.com/gold_nanorods.asp

[12] "6msx, iron containing ferritin at 1.43a." [Online]. Available: https://www.rcsb.org/3d-view/6MSX

[13] J. Waxenegger, A. Trugler, and U. Hohenester, "Plasmonics simulations with the mnpbem toolbox: Consideration of substrates and layer structures," *Computer Physics Communications*, vol. 193, pp. 138–150, 2015. [Online]. Available: https://www.sciencedirect.com/science/article/pii/S0010465515001228

[14] "Ferritin from equine spleen." [Online]. Available: https://www.sigmaaldrich.com/NL/en/product/sigma/f4503

[15] N. Galvez, B. Fernandez, P. Sanchez, R. Cuesta, M. Ceolin, M. Clemente-Leon, S. Trasobares, M. Lopez-Haro, J. J. Calvino, O. Stephan, and J. M. Dominguez-Vera, "Comparative structural and chemical studies of ferritin cores with gradual removal of their iron contents," *Journal of the American Chemical Society*, vol. 130, no. 25, pp. 8062–8068, 2008. [Online]. Available: https://doi.org/10.1021/ja800492z

[16] "Optical constants of Fe2O3." [Online]. Available: https://refractiveindex.info/?shelf=main&book=Fe2O3&page=Querry-o

Appendix A

Setup parts

1. DL pro diode laser from toptica: a tunable diode laser with digital control for a wavelength range of 785 $\pm$ 25 nm.
2. Bandpass (BP) filter, for wavelengths 785 $\pm$ 25 nm.
3. Polarizer: The polarization can be changed to increase or decrease the laser intensity. By changing it from 0 to 40 degrees, changes it from lowest to highest intensity respectively.
4. Single mode polarization stable optical fiber: an optical fiber to transmit a single wavelength while keeping polarization.
5. Glan-Thompson prism: a polarizing beam splitter.
6. Rotatable half-wave plate (HWP): This HWP changes the polarization of the light source to the specified angle.
7. 10(R):90(T) Beam splitter (BS): A BS where the reflection is 10% and the transmission 90%.
8. M1 and M2: are silver mirrors.
9. Objective (UPLFLN100XOP): magnification 100x, Numerical aperture (NA) is 1.3, working distance 0.2 mm, lens field of view 26.5 mm, coverglass thickness 0.17 mm, and be used with an immersion oil medium.
10. Sample holder: contains the prepared sample in a holder (sample preparation is described at B). A solution can be added on top of the holder, this will be measured.

11. Reference photodetector (PDA36A2): An amplified, switchable-gain, silicon (Si) photodetector, designed for light signals ranging from 350 nm to 1100 nm.
12. 50:50 Beam splitter (BS): used to split a light source 50:50 both ways.
13. Multimode polarization maintaining optical fiber: an optical fiber to transmit a wavelength range while keeping the polarization.
14. Laser-driven light source (model EQ-99 LDLS): a light source with a wavelength spectrum of 170 nm to 2500 nm.
15. Confocal and convex lenses.
16. 200 μm diameter pinhole.
17. APD430x from Thorlabs: an avalanche photodetector with adjustable gain.

Appendix B

Sample preparation

The process of creating the samples are discussed here, in 4 separate parts. First the cleaning of the coverglasses. Then the ozone cleaning of the coverglass and Gold NR preparation. Lastly the immobilization process of the gold NR to the coverglass.

B.0.1 Coverglass cleaning

1. We use coverglasses of borosilicate glass of 25 mm in diameter and thickness no.1.
2. The coverglasses are put in the holder.
3. The holder is put into the cup that is filled with acetone, and covered with aluminum (making sure no dust can come in).
4. Than the cup is sonicated for at least 20 minutes.
5. Next the acetone is removed and the holder/coverglasses are rinsed with water.
6. After the rinsing the holder is resuspended in ethanol and sonicated for at least 15 minutes.
7. Now the cup can be stored and used in the following processes.

B.0.2 Ozone cleaning the coverglass

1. The stored coverglasses are sonicated in the ethanol suspension for 5-10 minutes before use.

2. Single coverglasses are removed from the holder with tweezers and rinsed with water.
3. The slides are then dried with nitrogen pressured air.
4. Lastly they are ozone-cleaned for 1 hour.

B.0.3 Gold NR preparation

1. Pipet 300 μL of NR sample together with 700 μL of water into a test tube with lid.
2. Centrifuge the test tube for 2:00 minutes on 10,000 rpm.
3. Carefully remove the test tube from the centrifuge and remove 1000 μL from the test tube, removing the CTAB from the NR sample.
4. Them resuspend the NR in 100 μL of water, and sonicate the test tube for 40 minutes to 1 hour.

During sonication of the test tube containing the GNR, it is crucial to prevent the water in the sonication bath from becoming excessively warm. This can be verified by using touch as a method of assessment.

B.0.4 Immobilization process of the gold NR

1. Get the coverglasses from the ozone cleaner and put them on the spin coating machine.
2. Pipet the 100 μL of NR fluid in the center on the coverglass.
3. Then run spin coating, 300 rpm for 5 seconds, then 2000 rpm for 60 seconds, and lastly 4000 for $\approx$ 5 or 10 seconds
4. Remove the coverglass from the spin coater and lightly rinse with water.
5. Dry coverslip with pressured nitrogen and place the coverslip back into the ozone cleaner for 30 minutes.
6. Submerge the sample holder in ethanol and sonicated for 10-15 minutes.
7. Then rinse the sample holder with water, and dry it with nitrogen-pressured air.

8. Get the coverglass with NR from the ozone cleaner and heat at 70 degrees for 30 seconds.
9. Now the coverglass with NR can be placed into the sample holder.
10. Add 400 μL water on top to submerge the NR's.

Appendix C

NR spectra

Shows the spectra of the 3 NR used.

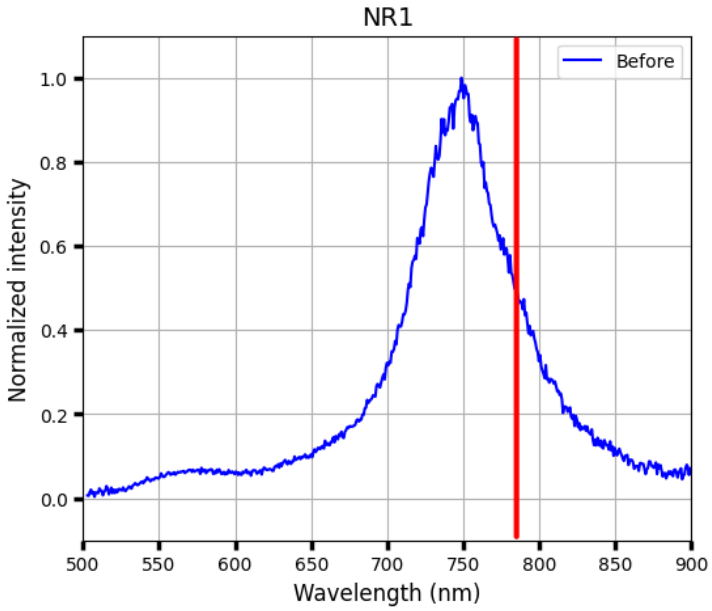

Figure C.1: *Spectra of NR1 before (blue) the measurements. The red line indicates the probing frequency of 785 nm*

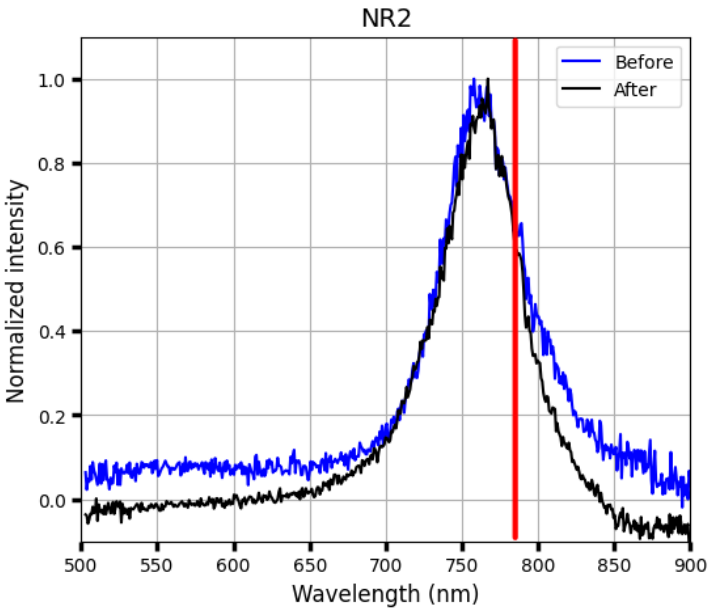

Figure C.2: *Spectra of NR2 before (blue) and after (black) the measurements. The red line indicates the probing frequency of 785 nm*

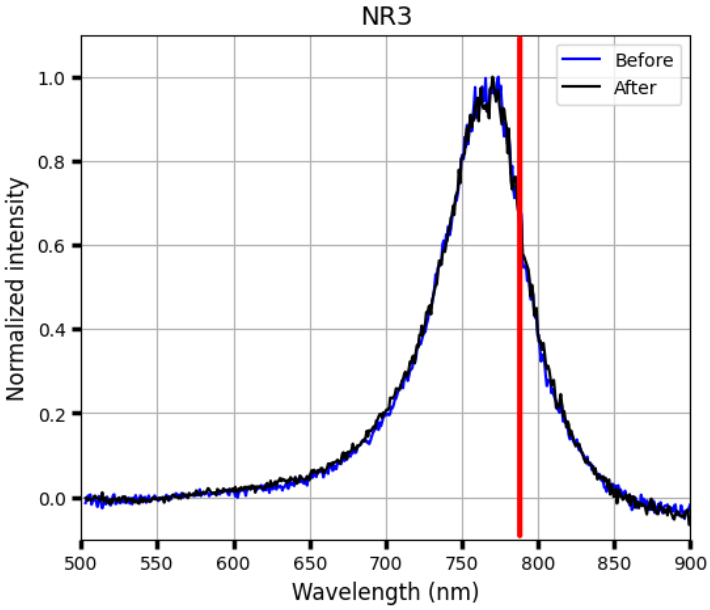

Figure C.3: *Spectra of NR3 before (blue) and after (black) the measurements. The red line indicates the probing frequency of 785 nm*

Version of July 7, 2023– Created July 7, 2023 - 13:03

Appendix D

Validation of the Labview code

Some changes have been made to the LabVIEW code, in terms of removing long-time fluctuation of the signal, this is only used when analyzing ferritin time trace signals. The change is in the method used for normalizing the long-time fluctuation of the signal, this will be explained in the next paragraph. Additionally, during the analysis, longer burst durations were occasionally separated due to the threshold setting, leading to the merging of two bursts within a specified distance

The previous code took the mean of specified bins from the trace and used these values for normalization. This works well when measuring short burst durations, but if the bursts are in the order of ms it will no longer work. The LabVIEW code developed performs the following tasks: it identifies the bursts, assigns them a lower weight, and applies a B-spline fit to the data, taking into account these weights. As a result, the bursts have a diminished impact on the overall B-spline fit.

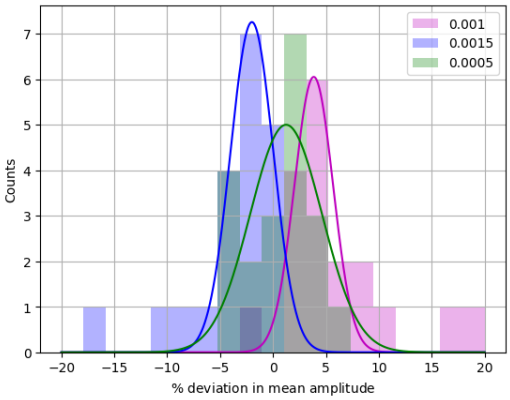

Figure D.1: *Histogram of the % deviation in mean amplitude for burst amplitudes of 0.001, 0.0015, and 0.0005.*

To validate the effectiveness of the new normalization method implemented to remove long-time signal fluctuations, simulated bursts were processed using the new LabVIEW code. Bursts are created with random locations and random duration between 1 - 1000 μs. They have been cre-

ated on a sinus wave with varying offsets between 0.1 and 1.8 V in amplitude. To this wave, Gaussian distributed noise is applied for a more accurate representation of the measured trace. This noise has a standard deviation of 0.0007, this is based on the standard deviation determined from measured time traces. Figure D.1 displays the percentage deviation in mean amplitude, for burst amplitudes of 0.001, 0.0015, and 0.0005. Resulted in 3.85, 1.99, and 1.24 % mean deviation for burst amplitudes of 0.001, 0.0015, and 0.0005 respectively.

It is important to note that when using this code it is only meant for ferritin bursts of longer duration. During the measurement, the threshold for burst detection needs to be adjusted, depending on the expected amplitude and noise level.

Version of July 7, 2023– Created July 7, 2023 - 13:03